Tunable Fano effect in parallel-coupled double quantum dot system

Haizhou Lu,[1,*] Rong Lü,[1] and Bang-fen Zhu[1,2,†]
[1]*Center for Advanced Study, Tsinghua University, Beijing 100084, China*
[2]*Department of Physics, Tsinghua University, Beijing 100084, China*
(Received 10 March 2005; revised manuscript received 21 April 2005; published 23 June 2005)

With the help of the Green function technique and the equation of motion approach, the electronic transport through a parallel-coupled double quantum dot (DQD) is theoretically studied. Owing to the interdot coupling, the bonding and antibonding states of the artificial quantum-dot molecule may constitute an appropriate basis set. Based on this picture, the Fano interference in the conductance spectra of the DQD system is readily explained. The possibility of manipulating the Fano line shape in the tunneling spectra of the DQD system is explored by tuning the dot-lead coupling, the interdot coupling, the magnetic flux threading the ring connecting dots and leads, and the flux difference between two subrings. It has been found that by making use of various tunings, the direction of the asymmetric tail of Fano line shape may be flipped by external fields and the continuous conductance spectra may be magnetically manipulated with the line shape retained. More importantly, by adjusting the magnetic flux, the function of two molecular states can be exchanged, giving rise to a swap effect, which might play a role as a qubit in the quantum computation.

DOI: 10.1103/PhysRevB.71.235320 PACS number(s): 73.63.Kv, 73.23.Hk, 73.40.Gk

I. INTRODUCTION

When the phase coherence of electrons passing through a mesoscopic system is retained, a number of quantum interference phenomena will occur. Recent advances in nanotechnologies have attracted much attention to the quantum coherence phenomena in the resonant tunneling processes of the quantum dot (QD) systems,[1] in which the typical length scale can be shorter than or comparable to the mean free path of electrons and the wave nature of electrons plays a decisive role. In the past decade, the widely adopted method of studying the phase coherence of a traversing electron through a QD is to measure the magnetic-flux-dependent current through an Aharonov-Bohm (AB) interferometer by inserting the QD into one of its arms.[2] The observed magnetic oscillation of the current will be the indication of the coherent transport through the QD, provided that at least partial coherence of electrons is kept.[3–13]

Fano resonance is another good probe for phase coherence in the QD system.[12–16] It is known that the Fano resonance stems from quantum interference between resonant and nonresonant processes,[17] and manifests itself in spectra as an asymmetric line shape in a large variety of experiments. Unlike the conventional Fano resonance,[18–21] the Fano effect in the QD system has its advantage in that its key parameters can be readily tuned. Suppose that a discrete level inside the QD acts as a Breit-Wigner-type scatter and is broadened by a factor of Γ due to couplings with the continua in leads. The key to realize the Fano effect in the conductance spectra is that, within Γ, the phase of the electron should smoothly change by π on the resonance.[8] The first observation of the Fano line shape in the QD system was reported by Göres *et al.*[14,15] in the single-electron-transistor experiments. Recently, Kobayashi *et al.* carried out research on magnetically and electrostatically tunable Fano effects in a QD embedded in an AB ring,[12,13] and Johnson *et al.* investigated a tunable Fano interferometer consisting of a QD coupled to a one-dimensional channel via tunneling and observed the Coulomb-modified Fano resonances.[16]

The double quantum dot (DQD) system, including the series-coupled DQD (Refs. 22–25), and parallel-coupled DQD (Refs. 3–6 and 26), makes the quantum transport phenomena rich and varied. The parallel-coupled DQD system is of particular interest, in which two QD's are, respectively, embedded into opposite arms of the AB ring, coupled to each other via barrier tunneling and coupled to two leads roughly equally. As a controllable two-level system, it is appealing for the parallel-coupled DQD system to become one of the promising candidates for the quantum bit in quantum computation based on solid-state devices.[27,28] The entangled quantum states required for performing the quantum computation demand a high degree of phase coherence in the system.[29] Being a probe of phase coherence,[30] if the Fano effect in the parallel-coupled DQD system is tunable and exhibits the swap effect, it is certainly of practical importance.

Inspired by recent experimental advances in the parallel DQD,[3–6,26] several groups have attempted to address this multipath system theoretically and predicted the Fano resonance in the parallel DQD system both with and without the interdot coupling.[31–37] For example, Kubala and König have studied the DQD with no interdot coupling.[31] In their model, for the two nondegenerate dots, the transport through dot 2 will provide a nonresonant channel for the resonant tunnel through dot 1, leading to the Fano resonance around the energy level of dot 1. Meanwhile, de Guevara *et al.* have studied the electronic transport through a DQD with the interdot coupling and found a progressive evolution of the tunneling through the antibonding state of the DQD molecule when the DQD system undergoes a transition from serial to parallel geometry.[33] However, it seems to the present authors that a physically transparent picture for the Fano effect in the parallel-coupled DQD system is still lacking, in particular what the resonant and nonresonant channels are in this Fano system. Moreover, a systematic study is required for exploring various possibilities of tuning the Fano effect with exter-

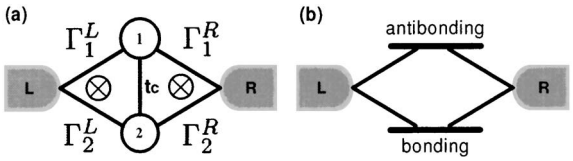

FIG. 1. (a) Schematic diagram for a tunneling-coupled parallel DQD system. (b) Schematic diagram of the parallel-coupled DQD system in the molecular orbital representation.

nal fields. In this paper, we intend to provide a natural yet simple explanation for the Fano effect in the parallel-coupled DQD and propose several ways to control the Fano resonance in the conductance spectra by the electrostatic and magnetic approaches.

The paper is organized as follows. In Sec. II, a widely used two-level Fano-Anderson model is introduced with an interdot coupling term added. Since the coupled quantum dots may be considered as an artificial QD molecules,[38] an effective Hamiltonian in terms of the bonding and antibonding states of the QD molecule may form an appropriate working basis. Thus with the help of the Green function technique and the equation of motion method,[39] the density of states (DOS) is calculated in three asymmetric configurations classified according to the spatial symmetry of the dot-lead coupling.[40] In Sec. III, the conductance formula is derived for this system,[41,42] whereby the Fano line shape in the conductance spectra is calculated in the absence of the magnetic flux. In Sec. IV, a simple mechanism explaining the Fano line shape in the DQD conductance spectrum is presented. Then, the possibilities of tuning the conductance line shape by various electrostatic and magnetic methods are described in detail, and several novel effects are predicted. Most importantly, by tuning the total magnetic flux, or the flux difference between the left and right parts of the AB ring, the swap effect between two resonance peaks in the conductance spectra is predicted, which might be of potential application as a type of C-NOT gate in the quantum computation. Finally, a brief summary is drawn and presented.

II. PHYSICAL MODEL

We start with the Fano-Anderson model for the parallel-coupled DQD where the discrete states in two quantum dots are coupled each other via tunneling. [Fig. 1(a)]. Then the Hamiltonian reads

$$H = H_{leads} + H_{DD} + H_T. \tag{1}$$

The H_{leads} in Eq. (1) represents the noninteracting electron gas in the left (L) and right (R) leads,

$$H_{leads} = \sum_{k,\alpha=L,R} \varepsilon_{k\alpha} c_{k\alpha}^{\dagger} c_{k\alpha}, \tag{2}$$

where, $c_{k\alpha}^{\dagger}$ and $c_{k\alpha}$ are the creation and annihilation operators for a continuum in the lead α with energy $\varepsilon_{k\alpha}$. The H_{DD} in Eq. (1) describes the QD electrons and their mutual coupling in the DQD—i.e.,

$$H_{DD} = \sum_{i=1,2} \varepsilon_i d_i^{\dagger} d_i - t_c e^{i\theta} d_1^{\dagger} d_2 - t_c e^{-i\theta} d_2^{\dagger} d_1. \tag{3}$$

The first term in Eq. (3), $d_i^{\dagger}$ (d_i), represents the creation (annihilation) operator of the electron with energy ε_i in the dot i. The second and third terms in Eq. (3) denote the interdot coupling, in which t_c is the coupling strength taken as a real parameter, and θ denotes a phase shift related to the flux difference between the left and right subrings. The H_T in Eq. (1) represents the tunneling coupling between the QD and lead electrons,

$$H_T = \sum_{k,\alpha=L,R} \sum_{i=1,2} V_{\alpha i} d_i^{\dagger} c_{k\alpha} + \text{H.c.}, \tag{4}$$

where the tunneling matrix element $V_{L1} = |V_{L1}| e^{i\phi/4}$, $V_{L2}^* = |V_{L2}| e^{i\phi/4}$, $V_{R1}^* = |V_{R1}| e^{i\phi/4}$, and $V_{R2} = |V_{R2}| e^{i\phi/4}$. Here, for the sake of simplicity, $V_{\alpha i}$ is assumed to be independent of k, and the phase shift due to the total magnetic flux threading into the AB ring, ϕ, is assumed to distribute evenly among four sections of the DQD-AB ring: namely, $\phi = 2\pi(\Phi_R + \Phi_L)/\Phi_0$, where the flux quantum $\Phi_0 = hc/e$. Thus, $\theta = \pi(\Phi_R - \Phi_L)/\Phi_0$. In the following calculation, we define the linewidth matrix as $\Gamma_{ij}^{\alpha} = \Sigma_k V_{\alpha i} V_{\alpha j}^* 2\pi\delta(\varepsilon - \varepsilon_{k\alpha})$ ($\alpha = L, R$) and $\mathbf{\Gamma} = \mathbf{\Gamma}^L + \mathbf{\Gamma}^R$. According to Fig. 1(a), the linewidth matrices in the QD representation read

$$\mathbf{\Gamma}^L = \begin{pmatrix} \Gamma_1^L & \sqrt{\Gamma_1^L \Gamma_2^L} e^{i\phi/2} \\ \sqrt{\Gamma_1^L \Gamma_2^L} e^{-i\phi/2} & \Gamma_2^L \end{pmatrix}$$

and

$$\mathbf{\Gamma}^R = \begin{pmatrix} \Gamma_1^R & \sqrt{\Gamma_1^R \Gamma_2^R} e^{-i\phi/2} \\ \sqrt{\Gamma_1^R \Gamma_2^R} e^{i\phi/2} & \Gamma_2^R \end{pmatrix}, \tag{5}$$

where Γ_i^{α} is short for Γ_{ii}^{α}.

To make the physical picture clearer and formalism simpler, it is attractive to introduce a QD-molecule representation by transforming two tunneling-coupled QD levels into the bonding and antibonding states of the QD molecule. The operator for a molecule state can be expressed as a linear superposition of the QD operators as

$$\begin{pmatrix} f_+ \\ f_- \end{pmatrix} = \begin{pmatrix} \cos\beta e^{-i\theta} & -\sin\beta \\ \sin\beta & \cos\beta e^{i\theta} \end{pmatrix} \begin{pmatrix} d_1 \\ d_2 \end{pmatrix}, \tag{6}$$

where f_- and f_+ are referred to as the annihilation operators for the bonding and antibonding states of the artificial QD molecule and the parameter β is defined as $\beta = 1/2 \tan^{-1}[2t_c/(\varepsilon_1 - \varepsilon_2)]$. For mathematical simplicity, in the following only the symmetric case is studied—i.e., $\varepsilon_1 = \varepsilon_2 = \varepsilon_0$, and thus $\beta = \pi/4$. Then the Hamiltonian for coupled dots is decoupled as

$$\tilde{H}_{DD} = (\varepsilon_0 + t_c) f_+^{\dagger} f_+ + (\varepsilon_0 - t_c) f_-^{\dagger} f_-. \tag{7}$$

In the molecular-state representation, the tunneling Hamiltonian between the leads and DQD is rewritten as

$$\tilde{H}_T = \sum_{k,\alpha=L,R} \sum_{i=+,-} \tilde{V}_{\alpha i} f_i^{\dagger} c_{k\alpha} + \text{H.c.}, \tag{8}$$

where the effective tunneling matrix elements are

$$\begin{pmatrix} \tilde{V}_{\alpha+} \\ \tilde{V}_{\alpha-} \end{pmatrix} = \frac{1}{\sqrt{2}} \begin{pmatrix} e^{-i\theta} & -1 \\ 1 & e^{i\theta} \end{pmatrix} \begin{pmatrix} V_{\alpha 1} \\ V_{\alpha 2} \end{pmatrix}. \tag{9}$$

Now, the DQD system has been mapped onto a system of two independent molecular states, which are connected to leads, respectively [cf. Fig. 1(b)]. In the molecular-state representation, the linewidth matrices read

$$\tilde{\Gamma}^{\alpha}_{ij} = \sum_k \tilde{V}_{\alpha i} \tilde{V}^{*}_{\alpha j} 2\pi \delta(\varepsilon - \varepsilon_{k\alpha}), \tag{10}$$

i.e.,

$$\tilde{\mathbf{\Gamma}}^{L} = \frac{1}{2} \begin{pmatrix} \Gamma_1^L + \Gamma_2^L - 2\sqrt{\Gamma_1^L \Gamma_2^L} \cos\left(\frac{\phi}{2} - \theta\right) & (\Gamma_1^L - \Gamma_2^L) e^{-i\theta} + \sqrt{\Gamma_1^L \Gamma_2^L} e^{i(\phi/2 - 2\theta)} - \sqrt{\Gamma_1^L \Gamma_2^L} e^{-i\phi/2} \\ (\Gamma_1^L - \Gamma_2^L) e^{i\theta} + \sqrt{\Gamma_1^L \Gamma_2^L} e^{-i(\phi/2 - 2\theta)} - \sqrt{\Gamma_1^L \Gamma_2^L} e^{i\phi/2} & \Gamma_1^L + \Gamma_2^L + 2\sqrt{\Gamma_1^L \Gamma_2^L} \cos\left(\frac{\phi}{2} - \theta\right) \end{pmatrix}, \tag{11}$$

and

$$\tilde{\mathbf{\Gamma}}^{R} = \frac{1}{2} \begin{pmatrix} \Gamma_1^R + \Gamma_2^R - 2\sqrt{\Gamma_1^R \Gamma_2^R} \cos\left(\frac{\phi}{2} + \theta\right) & (\Gamma_1^R - \Gamma_2^R) e^{-i\theta} + \sqrt{\Gamma_1^R \Gamma_2^R} e^{-i(\phi/2 + 2\theta)} - \sqrt{\Gamma_1^R \Gamma_2^R} e^{i\phi/2} \\ (\Gamma_1^R - \Gamma_2^R) e^{i\theta} + \sqrt{\Gamma_1^R \Gamma_2^R} e^{i(\phi/2 + 2\theta)} - \sqrt{\Gamma_1^R \Gamma_2^R} e^{-i\phi/2} & \Gamma_1^R + \Gamma_2^R + 2\sqrt{\Gamma_1^R \Gamma_2^R} \cos\left(\frac{\phi}{2} + \theta\right) \end{pmatrix}. \tag{12}$$

To estimate the broadening of the molecular level due to its couplings to leads, let us first calculate the density of states for each state. The retarded Green function for the molecular state is defined as $G^r_{\pm} = -i\theta(t)\langle\{f_{\pm}(t), f^{\dagger}_{\pm}\}\rangle$. With the equation of motion approach,[39] we have

$$G^r_{\pm}(\varepsilon) = \frac{1}{\varepsilon - (\varepsilon_0 \pm t_c) + i(\Gamma_{\pm})}, \tag{13}$$

where the imaginary part of the self-energy is equal to

$$\Gamma_{\pm} = \frac{1}{2}(\tilde{\Gamma}^L_{\pm\pm} + \tilde{\Gamma}^R_{\pm\pm}). \tag{14}$$

The local density of states is defined as the imaginary part of the retarded Green function as

$$\rho_{\pm}(\varepsilon) = -(1/\pi)\mathrm{Im}\, G^r_{\pm}(\varepsilon) = \frac{1}{\pi} \frac{\Gamma_{\pm}}{[\varepsilon - (\varepsilon_0 \pm t_c)]^2 + (\Gamma_{\pm})^2}, \tag{15}$$

which is the Lorentzian peaked at the molecular level.

Three configurations for the DQD system according to the asymmetric couplings between two dots and leads[40] that we focus on are shown in Fig. 2: (a) structure 1, in which $\Gamma_1^L = \Gamma_2^R = 2\Gamma_2^L = 2\Gamma_1^R = \gamma$; (b) structure 2, in which $\Gamma_1^L = \Gamma_1^R = 2\Gamma_2^L = 2\Gamma_2^R = \gamma$; and (c) structure 3, where $\Gamma_1^L = \Gamma_2^L = 2\Gamma_1^R = 2\Gamma_2^R = \gamma$. Here the γ is taken as an energy unit. These typical structures for the DQD system are basic, yet convenient to analyze theoretically.

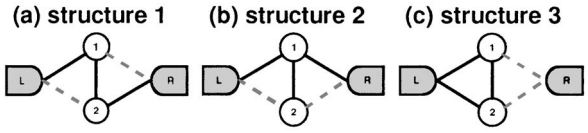

FIG. 2. Three structures investigated, in which the solid and dashed lines stand for the stronger and weaker tunnel couplings, respectively.

Figure 3 shows how the calculated DOS of two molecular states changes with the total magnetic flux ϕ in structures 1 and 2. It is noticed that structures 1 and 2 share the identical DOS. Two points are worth to pointing out. First, since the full width at half maximum $2\Gamma_{\pm}$ for each molecular state depends on the parameters Γ^{α}_i, ϕ, and θ, the broadenings of molecular states could be tuned not only by the dot-lead coupling strength and total magnetic flux, but also by the flux difference. Second, the broadening of one molecular state is always accompanied by the shrinking of the other molecular

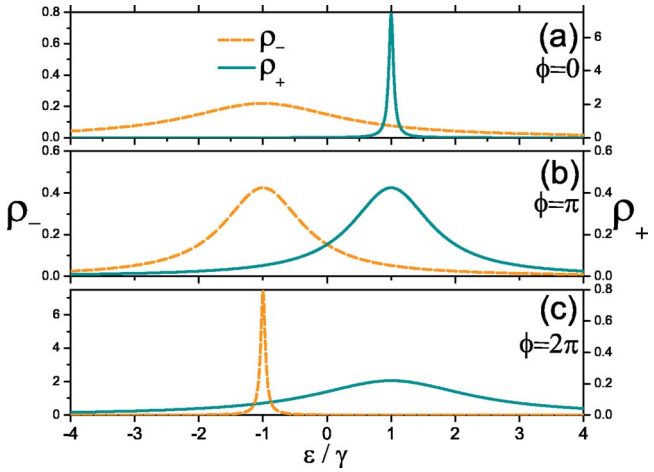

FIG. 3. (Color online) The density of states for two molecular states in structures 1 and 2 as shown in Fig. 2, where $t_c = \gamma$ which is taken as an energy scale.

state because the trace of the matrix of $(\tilde{\mathbf{\Gamma}}^L+\tilde{\mathbf{\Gamma}}^R)$ is an invariant, as explicitly shown by Eqs. (11) and (12). Third, in the absence of magnetic flux ($\phi=0$), $\Gamma_+\to 0^+$ in structure 3—i.e., the antibonding state—is totally decoupled from the leads and possesses an infinite lifetime. The finite ϕ introduced by the magnetic flux in this structure results in a finite coupling between the antibonding state and leads and, thus, a finite width for the antibonding state.

III. CONDUCTANCE

To study the transport through the DQD system, the conductance at zero temperature is derived, which, on the basis of the noninteracting molecular levels, can be reduced to the Landauer-Büttiker formula[41]

$$\mathcal{G}(\varepsilon)=\frac{2e^2}{h}T(\varepsilon), \tag{16}$$

where ε is the Fermi energy at both leads at equilibrium. In the absence of Coulomb interactions between the electrons on the dots, the transmission $T(\varepsilon)$ is expressed as[42]

$$T(\varepsilon)=\mathrm{Tr}[\mathbf{G}^a(\varepsilon)\mathbf{\Gamma}^R\mathbf{G}^r(\varepsilon)\mathbf{\Gamma}^L], \tag{17}$$

where the retarded and advanced Green functions $\mathbf{G}^r$ and $\mathbf{G}^a$ and the linewidth matrices $\mathbf{\Gamma}^{L(R)}$ can be expressed in molecular states representation or in dot levels representation, respectively.

The retarded Green function in the dot level representation is defined as $G^r_{ij}=-i\theta(t)\langle\{d_i(t),d_j^\dagger\}\rangle$, and its Fourier transformation $G^r_{ij}(\varepsilon)\equiv\langle\langle d_i|d_j^\dagger\rangle\rangle$ satisfies

$$\langle\langle d_i|d_j^\dagger\rangle\rangle=\delta_{ij}+\langle\langle[d_i,H]|d_j^\dagger\rangle\rangle, \tag{18}$$

which generates a closed set of linear equations for $G^r_{ij}(\varepsilon)$. The solution of $\mathbf{G}^r$ is given by

$$\mathbf{G}^r(\varepsilon)=\begin{pmatrix}\varepsilon-\varepsilon_1+\frac{i}{2}(\Gamma^L_{11}+\Gamma^R_{11}) & t_c+\frac{i}{2}(\Gamma^L_{12}+\Gamma^R_{12})\\ t_c^*+\frac{i}{2}(\Gamma^L_{21}+\Gamma^R_{21}) & \varepsilon-\varepsilon_2+\frac{i}{2}(\Gamma^L_{22}+\Gamma^R_{22})\end{pmatrix}^{-1}. \tag{19}$$

The advanced Green function is the Hermite conjugate of the retarded Green function. Put Eq. (19) into Eq. (17) and after some algebra, the transmission probability through the DQD system is found to be

$$T(\varepsilon)=\frac{a(\varepsilon-\varepsilon_0)^2+b(\varepsilon-\varepsilon_0)+c}{\{[\varepsilon-(\varepsilon_0+t_c)]^2+\Gamma_+^2\}\{[\varepsilon-(\varepsilon_0-t_c)]^2+\Gamma_-^2\}}, \tag{20}$$

where

$$\begin{aligned}a&=\Gamma_1^L\Gamma_1^R+\Gamma_2^L\Gamma_2^R+2\cos\phi\sqrt{\Gamma_1^L\Gamma_1^R\Gamma_2^L\Gamma_2^R},\\ b&=-2t_c(\Gamma_1^L+\Gamma_2^L)\sqrt{\Gamma_1^R\Gamma_2^R}\cos\left(\theta+\frac{\phi}{2}\right)\\ &\quad-2t_c(\Gamma_1^R+\Gamma_2^R)\sqrt{\Gamma_1^L\Gamma_2^L}\cos\left(\theta-\frac{\phi}{2}\right),\end{aligned} \tag{21}$$

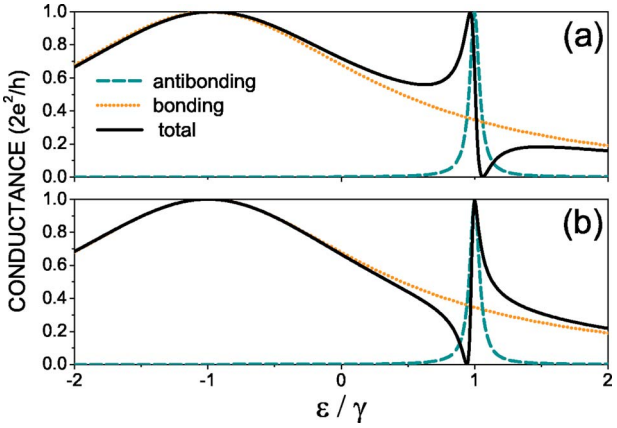

FIG. 4. (Color online) Conductance spectra in structures 1(a) and 2(b). The parameters for calculations are $\theta=0$, $\phi=0$, $\varepsilon_0=0$, and $t_c=\gamma$. Notice that the conductance spectra in two structures have quite different interference patterns though the identical DOS as in Fig. 3.

$$c=t_c^2(\Gamma_1^L\Gamma_2^R+\Gamma_2^L\Gamma_1^R+2\cos 2\theta\sqrt{\Gamma_1^L\Gamma_2^L\Gamma_1^R\Gamma_2^R}).$$

The conductance through the DQD system as expressed in Eq. (20) depends in general on the energy levels of two dots, dot-lead coupling, interdot coupling, and phase shift induced by the magnetic flux. Without the magnetic flux—i.e., $\phi=0$ and $\theta=0$—Eq. (20) recovers to the result by de Guevara *et al.*,[33] while in the limit of vanishing interdot coupling ($t_c=0$), the result of Kubala and König[31] is repeated.

In the molecular-state representation, the total conductance can also be divided into

$$\mathcal{G}_{\mathrm{total}}(\varepsilon)=\frac{2e^2}{h}\{T_+ + T_- + T_{\mathrm{inter}}\}, \tag{22}$$

where the transmission via each molecular state is

$$T_\pm(\varepsilon)=\frac{\tilde{\Gamma}^L_{\pm\pm}\tilde{\Gamma}^R_{\pm\pm}}{[\varepsilon-(\varepsilon_0\pm t_c)]^2+\Gamma_\pm^2} \tag{23}$$

and the interference term is given by

$$T_{\mathrm{inter}}=2\,\mathrm{Re}\left\{\frac{\tilde{\Gamma}^R_{+-}\tilde{\Gamma}^L_{-+}}{[\varepsilon-(\varepsilon_0+t_c)-i\Gamma_+][\varepsilon-(\varepsilon_0-t_c)+i\Gamma_-]}\right\}. \tag{24}$$

IV. TUNABLE FANO EFFECT

As shown in Fig. 4, the total conductance through the parallel-coupled DQD system consists of a Breit-Wigner peak and a Fano peak, which is quite different from the DOS where two Lorentzians are superposed. Based on the molecular level representation formulated above, let us first explain how the Fano interference is produced in some detail, then show how to tune it. Although similar observations have been reported in Refs. 32–34 and 36, it seems that until now no simple and transparent explanation has been available on the formation of the Fano line shape in this structure.

When a discrete level is buried into a continuum, the coupling between the discrete and continuous states gives rise to the renormalization of the states of whole system. The phase of the renormalized wave function varies by $\sim\pi$ swiftly as the energy transverses an interval $\sim\Gamma$ around the discrete level, where Γ is the broadening of the discrete level due to coupling with the continua.[17,43] Then, if there is a reference channel whose phase changes little in the interval of Γ around the discrete level, the quantum interference above and below the resonance level will be responsible for the Fano line shape in the conductance spectra—for example, the experimentally observed Fano line shape in the hybrid system of a QD and a reference arm.[12,13,16]

In the present DQD multipath system, it is not simple to identify the resonant and the reference channel. But on the basis of the molecular level representation, it is straightforward to interpret the Fano resonance in the DQD system in terms of the interference between two channels.

Usually, two molecular levels are coupled to the leads unequally. In the absence of magnetic flux, Eq. (14) simply reduces to

$$\Gamma_{\pm} = \frac{1}{4}(\Gamma_1^L + \Gamma_2^L + \Gamma_1^R + \Gamma_2^R) \mp \frac{1}{2}(\sqrt{\Gamma_1^L\Gamma_2^L} + \sqrt{\Gamma_1^R\Gamma_2^R}); \quad (25)$$

i.e., the broadening of one level is always accompanied by the shrinking of the other. The molecular level associated with a wider band can be referred to as the strongly coupled one, while that with narrow band is referred to as the weakly coupled level. Suppose that the broadening of the strongly coupled level entirely covers the bandwidth with the weakly coupled level and the phase shift for the strongly coupled channel is negligibly small around the weakly coupled level; then, a phase shift of π across the weakly coupled level can be detected with characteristic of the Fano line shape. Namely, the waves through two channels interfere constructively for electron with energy on one side of the weakly coupled level, while they interfere destructively on the other side. As a result, the Fano line shape shows up around the weakly coupled state. It is worth pointing out that the π phase shift also happens around the strongly coupled level, but on a energy scale much larger than that around the weakly coupled level (Fig. 3). That is why usually there is only one Fano peak around the weakly coupled level and the other peak around the strongly coupled level only exhibits little asymmetry.

Compared with the Fano effect in the hybrid system,[12,13,16] where the nonresonant channel served by a quantum point contact detects the π phase shift around the resonant tunneling channel through the QD, in the DQD system, the reference channel is the "less resonant" tunneling channel on one side of the strongly coupled level and the other "more resonant" channel through the weakly coupled level is accompanied with a swift π phase shift within a small energy region.

The Fano line shape in the present system can be tuned by the applied electrostatic and magnetic fields. Compared with the one-dot and one-arm case, where the magnetic field affects only the phase of the electron, but not the interaction strength,[12,13] in the parallel-coupled DQD, not only the phase but also the magnitude of the effective coupling between the molecular states and leads can be tuned by the magnetic flux. Of course, one should keep in mind that the interdot coupling is the prerequisite to the tunable Fano effect.

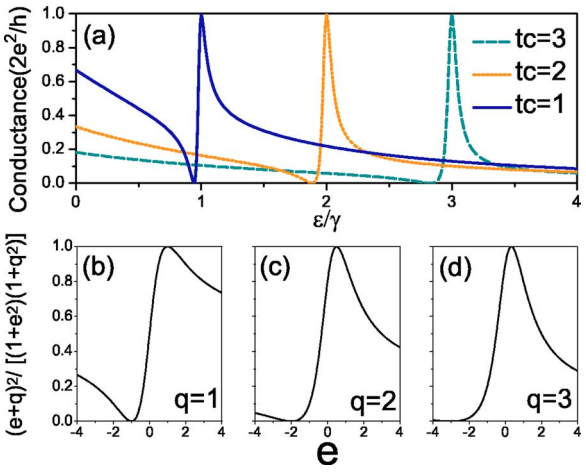

FIG. 5. (Color online) (a) Calculated conductance in structure 2 for three different values of the interdot coupling t_c, where the Fermi energy is roughly at the antibonding level. (b), (c), and (d) Simulation of the normalized Fano line shape with different asymmetric factors q as compared to the results obtained by Green functions in (a).

A. Electrostatic tuning

The interdot coupling t_c can be tuned by adjusting the height and thickness of the tunneling barrier between two dots through gate voltages and so can the dot-lead coupling $\Gamma_i^{L(R)}$.

The interference between the resonance and reference channels can be described as

$$\left| t_R \frac{\Gamma}{\omega - \epsilon_0 + i\Gamma} + t_N e^{i\phi} \right|^2 = t_N^2 \frac{|\tilde{\epsilon} + q|^2}{\tilde{\epsilon}^2 + 1}, \quad (26)$$

where t_R and t_N denote, respectively, the transmission amplitude via the resonance and reference channels, the detuning $\tilde{\epsilon} = (\omega - \epsilon_0)/\Gamma$, and the asymmetric factor $q = i + t_R e^{-i\phi}/t_N$. It is well known that when the asymmetric factor q is small, Eq. (26) gives rise to the asymmetric Fano line shape, while for large q, it tends to the symmetric Lorentzian. Figure 5(a) depicts the conductance spectra for three different interdot coupling strengths in structure 2. For comparison, the normalized Fano line shape [multiplied by a normalized factor $1/(1+q^2)$] is also plotted in Figs. 5(b), 5(c), and 5(d), demonstrating how the Fano line shape evolves with increasing q. It is obvious that as the interdot coupling increases, the bonding and antibonding splitting increases. As a result, the amplitude through the channel associated with the strongly coupled level but at the energy range of antibonding peak, t_N, decreases, and since q is inversely proportional to t_N, the asymmetric factor q increases. This further confirms our explanation above about the origin of Fano effect in this parallel-coupled DQD system.

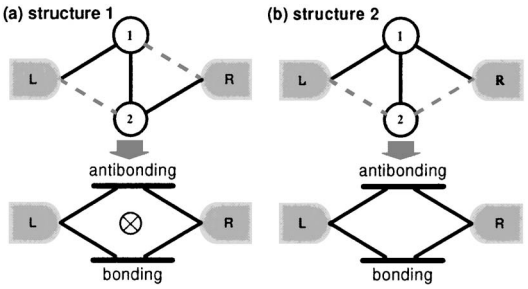

FIG. 6. (a) Structure 1 and (b) structure 2 can be cast into two different models of molecular states. The flux through the loop of structure 1 differs from that of structure 2 by a phase of π.

When tuning the dot-lead coupling strength $\Gamma_i^{L(R)}$ by tuning the gate voltage, the structure studied is changed, and the Fano line shape is changed accordingly. For example, when the strong and weak coupling in the linewidth matrix is adjusted such that structure 1 is transformed into structure 2 [see Fig. 4(b)], noticeably, the tail direction of the Fano peak is flipped. This delicate change can be understood in terms of the product of the effective tunneling matrix elements

$$\tilde{V}_{L+}\tilde{V}_{R+}^{*}\tilde{V}_{R-}\tilde{V}_{L-}^{*} = \frac{1}{4}(V_{L1}-V_{L2})(V_{R1}-V_{R2})(V_{L1}+V_{L2})(V_{R1}+V_{R2}). \quad (27)$$

In the wide band limit, a linewidth matrix element is proportional to the product of two dot-lead tunneling matrix elements. According to Fig. 2, the expression above for structure 1 differs from that for structure 2 by a minus sign, which implies that, compared to structure 2, an extra flux of π threads the loop in structure 1 (Fig. 6). Thus, the Fano line shape in structure 1 is just the opposite to that in structure 2—i.e., if two channels interfere with each other constructively in structure 1, then destructively in structure 2, and vice versa.

B. Magnetic flux tuning and swap operation

Coupled quantum dot systems have been proposed to materialize quantum-bits for quantum computation.[27] The swap operation is an important element to the controlled-NOT gate, which is the key to implementing the quantum computation.[44] Recently, a new mechanism has been proposed to realize the swap operation in the parallel-coupled DQD system by using the time-dependent interdot spin superexchange $J(t)$, which flips the singlet and triplet states formed by two localized electrons.[45] In the following we will discuss a new type of swap operation in the DQD system, which flips two quantum states by tuning the magnetic flux, including tuning the total flux ϕ or the flux difference 2θ between the left and right subrings. For the purpose of comparison, we only tune one parameter and let the other alone.

First, we tune the total flux ϕ and let $\theta=0$. When $\phi=(2n+1)2\pi$ (n is an integer), Eq. (14) turns out to be $\Gamma_{\pm}=\frac{1}{4}(\Gamma_1^L+\Gamma_2^L+\Gamma_1^R+\Gamma_2^R)\pm\frac{1}{2}(\sqrt{\Gamma_1^L\Gamma_2^L}+\sqrt{\Gamma_1^R\Gamma_2^R})$. Compared with the case of null flux, or $\phi=4n\pi$ [Eq. (25)], the widths of the bonding and antibonding states are interchanged. Figure 7 demonstrates the evolution of conductances with changing the total magnetic flux in three asymmetric configurations for zero θ. In this circumstance the Fano and Breit-Wigner peaks in the conductance spectra of structures 1 and 2 have been exchanged with each other, when changing ϕ from $(2n+1)2\pi$ to $\phi=4n\pi$. On the other hand, when $\phi=(2n+1)\pi$, two identical peaks appear in the conductance spectra symmetrically, which is quite similar to the DOS spectra. In structure 3, no Fano peak exists without the magnetic flux according to Eq. (15) and Fig. 7, because the antibonding state is totally decoupled from the leads. However, if ϕ deviates a little from zero or, more generally, from a multiple of 2π, the channel connecting the decoupled state and the leads is open, and the Fano interference comes back again. Our model calculation indicates that this flux-dependent Fano effect takes place whenever $\Gamma_1^L=\Gamma_2^L$ and $\Gamma_1^R=\Gamma_2^R$, regardless of whether the four dot-lead couplings are identical.[33]

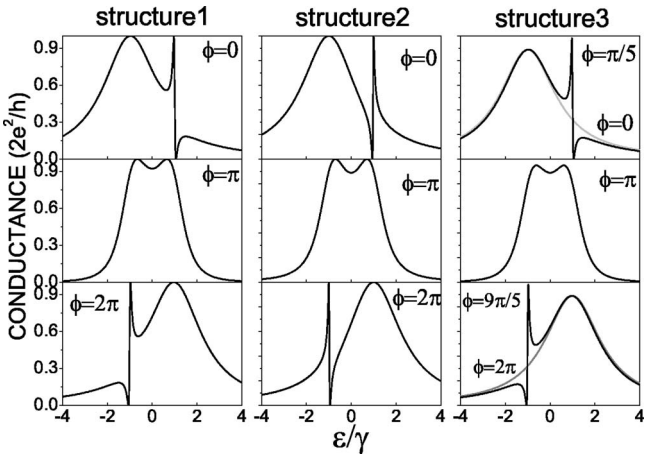

FIG. 7. The evolution of transmission spectrum with total magnetic flux ϕ tuned for three asymmetric configurations.

Tuning θ, half of the flux difference between the left and right subrings, can also lead to two resonance peak swap and the flux-dependent Fano effect as shown in Fig. 8. It is no-

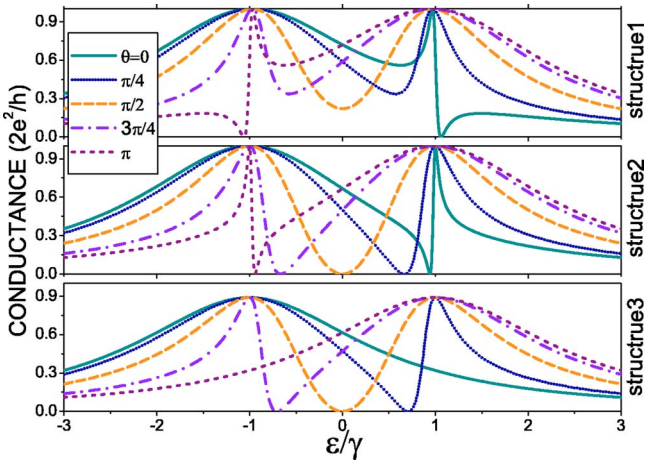

FIG. 8. (Color online) The evolution of transmission spectrum with phase difference θ in three asymmetric configurations.

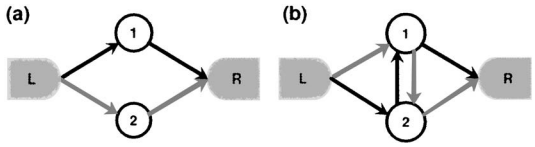

FIG. 9. Illustration for two different periods of conductance. Multipathway interference as functions of (a) the total flux ϕ and (b) the flux difference θ.

ticed when $\theta=\pi$, the results coincide with what obtained when $\phi=2\pi$.

It is interesting to note that the conductance oscillation is a periodic function of ϕ with a period of 4π and a periodic function of θ with a period of 2π. The difference in the period can be readily explained as the multipathway nature in this parallel-coupled DQD system. If an electron transits from the left to the right, it gathers a phase factor $e^{i(\phi/4+\phi/4)}=e^{i\phi/2}$ via the upper arms and $e^{-i\phi/2}$ via the lower arms [Fig. 9(a)]. The interference of the two paths gives $\cos(\phi/2)$, which is associated with a period of 4π. On the other hand, if two routes of an electron are illustrated as the arrows in Fig. 9(b), the interference yields $\cos\theta$ and the 2π periodicity, because the first path from the left lead $\rightarrow$ dot 1 $\rightarrow$ dot 2 $\rightarrow$ right lead accumulates a phase $e^{i(\phi/4+\theta-\phi/4)}=e^{i\theta}$ and the second symmetric route through dot2 $\rightarrow$ dot1 gives a phase $e^{-i\theta}$.

The quantum interference tuned by the magnetic flux in the DQD system makes the conductance to vary in some fancy way. Let us look at a peculiar instance, the continuous manipulation of the conductance with the line shape retained. In Fig. 10, two cases of the flux tuning are (1) $\phi=(2n+1)\pi$, $\theta\in[0,\pi/2]$ and (2) $\theta=(2n+1)\pi/2$, $\phi\in[0,\pi]$. According to Eqs. (11) and (12), once $\theta=(2n+1)\pi/2$ or $\phi=(2n+1)\pi$, the line shape of the DOS for two molecular levels is fixed. In our calculations, $\Gamma_1^L=\Gamma_2^L=\Gamma_1^R=\Gamma_2^R=t_c=\gamma$, $\varepsilon_0=0$, only a single peak appears in Fig. 10(a) (when increasing t_c, the conductance will recover the double-peak feature). In contrast, in Fig. 10(b), due to the destructive interference, the conductance at ε_0 is always zero. Besides, a fully symmetric configuration with four identical dot-lead couplings is considered in this calculation, so that the maximum and minimum values of the conductance are precisely at $2e^2/h$ and 0, respectively.

V. CONCLUSIONS

In summary, the transport through the parallel-coupled DQD system has been studied, in which a particular attention is paid to the mechanism of the Fano line shape in conductance spectra as well as its tunability. Due to the interdot coupling, a QD molecule is formed and can be the proper representation for the present investigations. Due to the coupling between the molecular levels and leads, two levels are broadened into two bands: one is wider, which is associated with the strongly coupled level, and the other narrower band is related to the weakly coupled level. When the wider band covers the narrower one and is associated with a negligible phase shift around the weakly coupled level, the π phase shift at resonance of the wave function of the narrower band may be detected via the quantum interference and shows up as the Fano line shape. Thus, both the reference and resonance channels for Fano interference are readily identified. Since the density of states and the effective couplings between the molecular levels and leads are tunable by making use of the magnetic flux and gate voltages, several ways to control the Fano line shape are proposed, including the total flux ϕ, the flux difference between two subrings θ, the interdot coupling strength t_c, and the dot-lead coupling. In these ways, we may realize the swap effect, the flipped tail direction of the Fano line shape, and the continuous line-shape-keeping magnetic switch in this DQD system, which might be of practical applications.

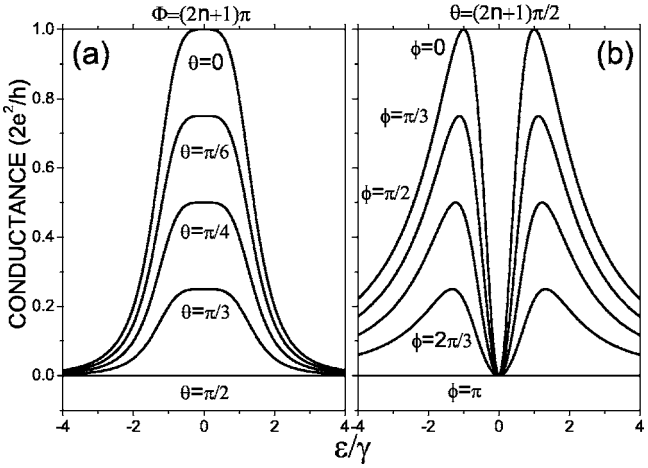

FIG. 10. Continuously modulated conductance by the magnetic flux. (a) The conductance is tuned by θ, when ϕ is fixed at $(2n+1)\pi$. (b) The conductance is tuned by ϕ, when $\theta=(2n+1)\pi/2$.

ACKNOWLEDGMENTS

We would like to acknowledge Hui Zhai, Zuo-zi Chen, and Chaoxing Liu for helpful discussions. This work is supported by the Natural Science Foundation of China (Grant No. 10374056), the MOE of China (Grant No. 2002003089), and the Program of Basic Research Development of China (Grant No. 2001CB610508).

*Electronic address: luhz@castu.tsinghua.edu.cn
†Electronic address: bfzhu@castu.tsinghua.edu.cn

[1] L. P. Kouwenhoven, C. M. Markus, P. L. McEuen, S. Tarucha, R. M. Westervelt, and N. S. Wingreen, in *Mesoscopic Electon Transport*, edited by L. L. Sohn, L. P. Kouwenhoven, and G. Schön, Vol. 345 of *NATO Advanced Study Institute, Ser. E* (Kluwer, Dordrecht, 1997).
[2] Y. Aharonov and D. Bohm, Phys. Rev. **115**, 485 (1959).
[3] A. W. Holleitner, C. R. Decker, H. Qin, K. Eberl, and R. H. Blick, Phys. Rev. Lett. **87**, 256802 (2001).
[4] A. W. Holleitner, R. H. Blick, A. K. Hüttel, K. Eberl, and J. P. Kotthaus, Science **297**, 70 (2002).
[5] A. W. Holleitner, R. H. Blick, and K. Eberl, Appl. Phys. Lett. **82**, 1887 (2003).
[6] R. H. Blick, A. K. Hüttel, A. W. Holleitner, E. M. Höhberger, H. Qin, J. Kirschbaum, J. Weber, W. Wegscheider, M. Bichler, K. Eberl, and J. P. Kotthaus, Physica E (Amsterdam) **16**, 76 (2003).
[7] A. Yacoby, M. Heiblum, D. Mahalu, and H. Shtrikman, Phys. Rev. Lett. **74**, 4047 (1995).
[8] R. Schuster, E. Buks, M. Heiblum, D. Mahalu, V. Umansky, and H. Shtrikman, Nature (London) **385**, 417 (1997).
[9] E. Buks, R. Schuster, M. Heiblum, D. Mahalu, and V. Umansky, Nature (London) **391**, 871 (1998).
[10] W. G. van der Wiel, S. De Franceschi, T. Fujisawa, J. M. Elzerman, S. Tarucha, and L. P. Kouwenhoven, Science **289**, 2105 (2000).
[11] Y. Ji, M. Heiblum, D. Sprinzak, D. Mahalu, and H. Shtrikman, Science **290**, 779 (2000).
[12] K. Kobayashi, H. Aikawa, S. Katsumoto, and Y. Iye, Phys. Rev. Lett. **88**, 256806 (2002).
[13] K. Kobayashi, H. Aikawa, S. Katsumoto, and Y. Iye, Phys. Rev. B **68**, 235304 (2003).
[14] J. Göres, D. Goldhaber-Gordon, S. Heemeyer, M. A. Kastner, H. Shtrikman, D. Mahalu, and U. Meirav, Phys. Rev. B **62**, 2188 (2000).
[15] I. G. Zacharia, D. Goldhaber-Gordon, G. Granger, M. A. Kastner, Y. B. Khavin, H. Shtrikman, D. Mahalu, and U. Meirav, Phys. Rev. B **64**, 155311 (2001).
[16] A. C. Johnson, C. M. Marcus, M. P. Hanson, and A. C. Gossard, Phys. Rev. Lett. **93**, 106803 (2004).
[17] U. Fano, Phys. Rev. **124**, 1866 (1961).
[18] R. K. Adair, C. K. Bockelman, and R. E. Peterson, Phys. Rev. **76**, 308 (1949).
[19] U. Fano and J. W. Cooper, Phys. Rev. **137**, A1364 (1965).
[20] F. Cerdeira, T. A. Fjeldly, and M. Cardona, Phys. Rev. B **8**, 4734 (1973).
[21] J. Faist, F. Capasso, C. Sirtori, K. W. West, and L. N. Pfeiffer, Nature (London) **390**, 589 (1997).
[22] F. R. Waugh, M. J. Berry, D. J. Mar, R. M. Westervelt, K. L. Campman, and A. C. Gossard, Phys. Rev. Lett. **75**, 705 (1995).
[23] R. H. Blick, D. Pfannkuche, R. J. Haug, K. v. Klitzing, and K. Eberl, Phys. Rev. Lett. **80**, 4032 (1998).
[24] T. H. Oosterkamp, T. Fujisawa, W. G. van der Wiel, K. Ishibashi, R. V. Hijman, S. Tarucha, and L. P. Kouwenhoven, Nature (London) **395**, 873 (1998).
[25] H. Qin, A. W. Holleitner, K. Eberl, and R. H. Blick, Phys. Rev. B **64**, 241302(R) (2001).
[26] J. C. Chen, A. M. Chang, and M. R. Melloch, Phys. Rev. Lett. **92**, 176801 (2004).
[27] D. Loss and D. P. DiVincenzo, Phys. Rev. A **57**, 120 (1998).
[28] X. Hu and S. Das Sarma, Phys. Rev. A **61**, 062301 (2000).
[29] D. P. DiVincenzo, in *Mesoscopic Electron Transport*, edited by L. L. Sohn, L. P. Kouwenhoven, and G. Schön, Vol. 345 of *NATO Advanced Study Institute, Ser. E* (Kluwer, Dordrecht, 1997).
[30] A. A. Clerk, X. Waintal, and P. W. Brouwer, Phys. Rev. Lett. **86**, 4636 (2001).
[31] B. Kubala and J. König, Phys. Rev. B **65**, 245301 (2002).
[32] K. Kang and S. Y. Cho, J. Phys.: Condens. Matter **16**, 117 (2004).
[33] M. L. Ladrón de Guevara, F. Claro, and Pedro A. Orellana, Phys. Rev. B **67**, 195335 (2003).
[34] Z.-M. Bai, M.-F. Yang, and Y.-C. Chen, J. Phys.: Condens. Matter **16**, 2053 (2004).
[35] B. Dong, I. Djuric, H. L. Cui, and X. L. Lei, J. Phys.: Condens. Matter **16**, 4303 (2004).
[36] P. A. Orelana, M. L. Ladrón de Guevara, and F. Claro, cond-mat/0404293 (unpublished).
[37] R. López, D. Sánchez, M. Lee, M.-S. Choi, P. Simon, and K. Le Hur, Phys. Rev. B **71**, 115312 (2005).
[38] C. Livermore, C. H. Crouch, R. M. Westervelt, K. L. Campman, and A. C. Gossard, Science **274**, 1332 (1996).
[39] H. Haug and A.-P. Jauho, *Quantum Kinetics in Transport and Optics of Semiconductors* (Springer-Verlag, Berlin, 1996).
[40] J. König and Y. Gefen, Phys. Rev. B **65**, 045316 (2002).
[41] S. Datta, *Electronic Transport in Mesoscopic Systems* (Cambridge University Press, Cambridge, England, 1997).
[42] Y. Meir and N. S. Wingreen, Phys. Rev. Lett. **68**, 2512 (1992).
[43] G. D. Mahan, *Many-Particle Physics*, 2nd ed. (Plenum Press, New York, 1990).
[44] D. P. DiVincenzo, Phys. Rev. A **51**, 1015 (1995).
[45] G.-M. Zhang, R. Lü, Z. R. Liu, and L. Yu, cond-mat/0403629 (unpublished).